

LINC01094 accelerates the metastasis of hepatocellular carcinoma *via* the miR-26b-3p/MDM4 axis

Yingmin Mao, Zhe Hu, Yunjian Zeng, Yuqi Zhou, Zili Shi*

Department of Interventional Therapy, Tongde Hospital of Zhejiang Province, Hangzhou, China

ARTICLE INFO

Original paper

Article history:

Received: March 15, 2023

Accepted: June 23, 2023

Published: June 30, 2023

Keywords:

LINC01094, miR-26b-3p, MDM4, HCC

ABSTRACT

To elucidate the role of LINC01094 in accelerating the metastatic potential of hepatocellular carcinoma (HCC) *via* the miR-26b-3p/MDM4 axis. Differential levels of LINC01094 in clinical samples of HCC and their influence on pathological indicators of recruited HCC patients were detected. Hep3B and SK-HEP-1 cell lines with stable knockdown of LINC01094 were generated by shRNA transfection, followed by detection of migration and invasion by Transwell and wound healing assay. Bioinformatic analysis, dual-luciferase reporter assay and rescue experiments were conducted to assess the interaction between LINC01094 and the miR-26b-3p/MDM4 axis. LINC01094 was upregulated in clinical samples of HCC and its level was linked to the incidences of lymphatic and distant metastasis of HCC patients. Knockdown of LINC01094 weakened migratory and invasive abilities in Hep3B and SK-HEP-1 cells. MiR-26b-3p was the downstream target of LINC01094, which was lowly expressed in HCC tissues and negatively correlated to the LINC01094 level. Moreover, MDM4 was the target gene of miR-26b-3p, which was highly expressed in HCC tissues and negatively correlated to the miR-26b-3p level. Rescue experiments showed that the knockdown of miR-26b-3p could reverse the inhibited metastasis in Hep3B and SK-HEP-1 cells with a stable knockdown of LINC01094. LINC01094 accelerates the metastasis of HCC *via* the miR-26b-3p/MDM4 axis, which is a potential biomarker and therapeutic target to be utilized in clinical practice.

Doi: <http://dx.doi.org/10.14715/cmb/2023.69.6.27>Copyright: © 2023 by the C.M.B. Association. All rights reserved. 

Introduction

Liver cancer is a malignant solid tumor that is highly prevalent in the world (1,2). In 2018, there were approximately 841,000 new cases and 782,000 deaths of liver cancer globally, and China is the high-incidence area for it (3,4). Hepatocellular carcinoma (HCC) covers most liver cancer cases (80-90%) (4,5). Although huge progress has been made in the diagnosis and treatment of HCC, its prognosis is unsatisfactory due to its highly metastatic and aggressive characteristics (5-7). Therefore, it is urgent to study the molecular mechanism of HCC and to explore effective biomarkers and therapeutic targets (8,9).

In recent years, a large number of non-coding RNAs have been discovered. They do not have the ability to encode proteins, but they participate in various physiological and pathological processes (10,11). At present, long non-coding RNAs (lncRNAs) and miRNAs are the most explored non-coding RNAs (12,13). lncRNAs have more than 200 nucleotides in length and they have limited protein-encoding potential (14,15). They are vital regulators in both the normal development of the body and pathological processes (14,16). Through literature review, the involvement of LINC01094 in HCC is rarely reported (17,18). Our previous research has demonstrated the highly abundant LINC01094 in HCC tissues, and its potential biological functions is further analyzed.

Through bioinformatic analysis, LINC01094/miR-26b-3p/MDM4 axis was identified. Previous evidences

have reported that miR-26b-3p and MDM4 are abnormally activated in tumor profile (19,20). In the present study, we mainly explore the involvement of the LINC01094/miR-26b-3p/MDM4 axis in affecting HCC metastasis.

Materials and Methods

HCC samples

Paired HCC and non-tumoral tissues were surgically resected from 36 HCC patients, labeled and stored at -80°C. The collection and use of clinical samples have been approved by the Ethics Committee of Tongde Hospital of Zhejiang Province. Recruited patients and their families have been fully informed that their tissue samples would be used for scientific research. All participating patients have signed informed consent. This study complied with the Helsinki Declaration.

Cell culture

Human HCC cell lines (Huh-7, Hep3B, SK-HEP-1 and MHCC-97H) and normal liver cell line (THLE-3) were provided by American Type Culture Collection (ATCC) (Manassas, VA, USA). Cells were cultured in Dulbecco's modified eagle medium (DMEM) and maintained in a humidified environment with 5% CO₂ at 37°C. 10% fetal bovine serum (FBS), 100 U/mL penicillin and 100 µg/mL streptomycin were added in the medium (Gibco, Rockville, MD, USA). Until cells were cultivated to 80-90% density, they were passaged using 1×trypsin+EDTA

* Corresponding author. Email: shizili1923@126.com

(ethylenediaminetetraacetic acid).

Transfection

Cells were inoculated in the 6-well plate and cultivated to 40-60% density. Transfection was conducted using Lipofectamine 2000 (Invitrogen, Carlsbad, CA, USA). After 48 h cell transfection, cells were collected for verifying transfection efficacy and functional experiments.

Transwell migration and invasion assay

The cell suspension was prepared at 5×10^5 cells/ml. 200 μ L of suspension and 700 μ L of medium containing 20% FBS were respectively added on the top and bottom of a Transwell insert, and cultured for 48 h. Migratory cells on the bottom were induced with methanol for 15 min, 0.2% crystal violet for 20 min and captured using a microscope. Five random fields per sample were selected for capturing and counting migratory cells. Invasion assay was similarly conducted in a Transwell insert pre-coated with diluted Matrigel (Sigma-Aldrich, St. Louis, MO, USA).

Wound healing assay

Cell suspension in serum-free medium was prepared at 5×10^5 /mL, and implanted in 6-well plates. Cells were cultivated to 90% density, followed by creating an artificial scratch using a sterilized pipette tip. Cells were washed in phosphate-buffered saline (PBS) 2-3 times and cultured in the medium containing 1% FBS. 24 hours later, wound closure percentage was calculated.

Quantitative real-time polymerase chain reaction (qRT-PCR)

Cells were lysed using TRIzol reagent (Invitrogen, Carlsbad, CA, USA) for isolating RNAs, which were purified for clearing genomic DNA using DNase I, and reversely transcribed to the first-strand of complementary deoxyribose nucleic acids (cDNAs) using Primescript RT Reagent (TaKaRa, Otsu, Japan). SYBR®Premix Ex Taq™ and StepOne Plus Real-time PCR system were utilized for qRT-PCR. (Table 1).

Western blot

Cells were lysed in radioimmunoprecipitation assay (RIPA) (Beyotime, Shanghai, China) on ice for 30 min and centrifuged at $14000 \times g$, $4^\circ C$ for 15 min. The concentration of cellular protein was determined by the bicinchoninic acid (BCA) method (Pierce, Rockford, IL, USA). Protein samples were separated by 10% sodium dodecyl sulphate-polyacrylamide gel electrophoresis (SDS-PAGE), and

loaded on a polyvinylidene fluoride (PVDF) membrane (Roche, Basel, Switzerland). The membrane was blocked in 5% skim milk for 2 h. They were incubated with primary and secondary antibodies, followed by band exposure.

Dual-luciferase reporter assay

Wild-type and mutant-type vectors were generated according to the predicted sites using online software. They were co-transfected to cells with miR-26b-3p mimic or NC mimic, respectively. On the other day, cells were lysed for measuring luciferase activity (Promega, Madison, WI, USA).

Statistical analysis

GraphPad Prism 5 V5.01 (La Jolla, CA, USA) was used for statistical analysis. Differences between groups were compared using the *t*-test. The potential influence of LINC01094 on pathological indicators of recruited HCC patients was analyzed by Chi-square test. The relationship between relative expressions of two genes in HCC tissues was determined by the Spearman correlation test. Data were expressed as mean \pm standard deviation. $P < 0.05$ was considered statistically significant.

Results

LINC01094 was highly expressed in HCC

qRT-PCR was conducted to detect the expression characteristics of LINC01094 in HCC tissues and cell lines. The results showed that LINC01094 was more highly expressed in HCC tissues than that adjacent non-tumoral ones (Figure 1A), suggesting that LINC01094 may play an ontogenetic role in HCC. In addition, compared to the normal liver cell line, LINC01094 was significantly upregulated in HCC cell lines (Figure 1B).

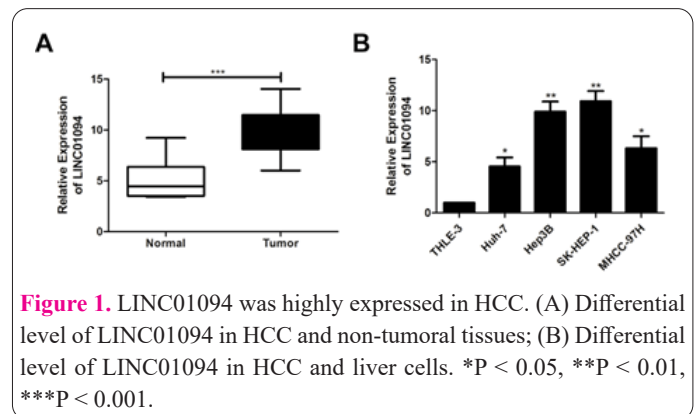


Table 1. Primer sequence.

Gene	Primer sequence
LINC01094	Forward: 5'-GCTTCTCCGTGAAAGACCCA-3'
	Reverse: 5'-GCTTCTCCGTGAAAGACCCA-3'
MDM4	Forward: 5'-GCTTCTCCGTGAAAGACCCA-3'
	Reverse: 5'-TCCTCTGCACCTTTGCTTCAGT-3'
GAPDH	Forward: 5'-GTCAAGGCTGAGAACGGGAA-3'
	Reverse: 5'-AAATGAGCCCCAGCCTTCTC-3'
miR-26b-3p	Forward: 5'-CAGCCTGTTCTCCATTACTTG-3'
	Reverse: 5'-GGTCCAGTTTTTTTTTTTTTTTAGC-3'
U6	Forward: 5'-CTCGCTTCGGCAGCAC-3'
	Reverse: 5'-AACGCTTCACGAATTTGCGT-3'

Table 2. Association of LINC01094 expression with clinicopathologic characteristics of hepatocellular carcinoma.

Parameters	Number of cases	LINC01094 expression		P-value
		Low (n=19)	High (n=17)	
Age (years)				0.317
<60	18	8	10	
≥60	18	11	7	
Gender				0.492
Male	17	10	7	
Female	19	9	10	
T stage				0.765
T1-T2	20	11	9	
T3-T4	16	8	8	
Lymph node metastasis				0.048
No	21	14	7	
Yes	15	5	10	
Distance metastasis				0.018
No	24	16	8	
Yes	12	3	9	

Subsequently, the relationship between LINC01094 level and pathological indicators of recruited HCC patients was analyzed by Chi-square test. It is found that LINC01094 had a close relation to the incidences of lymphatic and distant metastasis of HCC (Table 2).

Knockdown of LINC01094 weakened metastasis in HCC

SK-HEP-1 and Hep3B cell lines with stable knockdown of LINC01094 were generated by shRNA transfection. The transfection efficacy of sh-LINC01094#1 was the best among the three shRNAs and it was utilized in the following experiments (Figure 2A). Knockdown of LINC01094 remarkably reduced both migratory and invasive rates in SK-HEP-1 and Hep3B cells (Figure 2B, 2C). It is suggested that LINC01094 stimulated metastasis in HCC.

LINC01094 was bound to miR-26b-3p

Three miRNA candidates that were specifically bound to LINC01094 were searched from online bioinformatic software. Among them, the expression change of miR-26b-3p responded to the knockdown of LINC01094 and was the most pronounced (Figure 3A). MiR-26b-3p was detected to be downregulated in HCC cell lines and clinical samples (Figure 3B, 3C). Moreover, it was negatively linked to LINC01094 level in HCC tissues (Figure 3D). Transfection of sh-LINC01094#1 upregulated miR-26b-3p in SK-HEP-1 and Hep3B cells, consistently indicating their negative correlation (Figure 3E). In order to further verify the miRNA sponge effect of LINC01094 on miR-26b-3p, a dual-luciferase reporter assay was performed. As expected, LINC01094 could target miR-26b-3p through the predicted binding site (Figure 3F).

MDM4 was the target gene of miR-26b-3p

After searching the online database (miRDB, TargetScan and Starbase) and cross-match analysis, MDM4 was identified as the target gene of miR-26b-3p (Figure 4A). MDM4 was upregulated in HCC cell lines and clinical samples (Figure 4B, 4C). A negative correlation was dis-

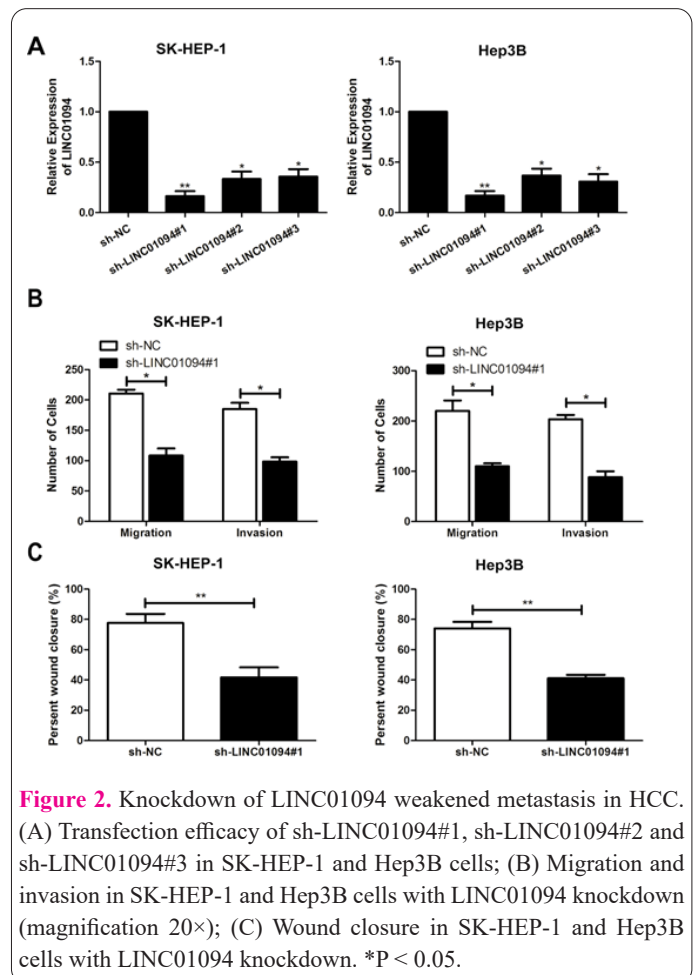


Figure 2. Knockdown of LINC01094 weakened metastasis in HCC. (A) Transfection efficacy of sh-LINC01094#1, sh-LINC01094#2 and sh-LINC01094#3 in SK-HEP-1 and Hep3B cells; (B) Migration and invasion in SK-HEP-1 and Hep3B cells with LINC01094 knockdown (magnification 20×); (C) Wound closure in SK-HEP-1 and Hep3B cells with LINC01094 knockdown. *P < 0.05.

covered between relative expressions of miR-26b-3p and MDM4 in HCC tissues (Figure 4D). Moreover, the protein level of MDM4 was downregulated by transfection of sh-LINC01094#1 in SK-HEP-1 and Hep3B cells, indicating a positive interaction between MDM4 and LINC01094 (Figure 4E, left). MDM4 was upregulated by transfection of miR-26b-3p inhibitor, confirming the negative interaction between MDM4 and miR-26b-3p (Figure 4E, right). Dual-luciferase reporter assay proved that MDM4 was the

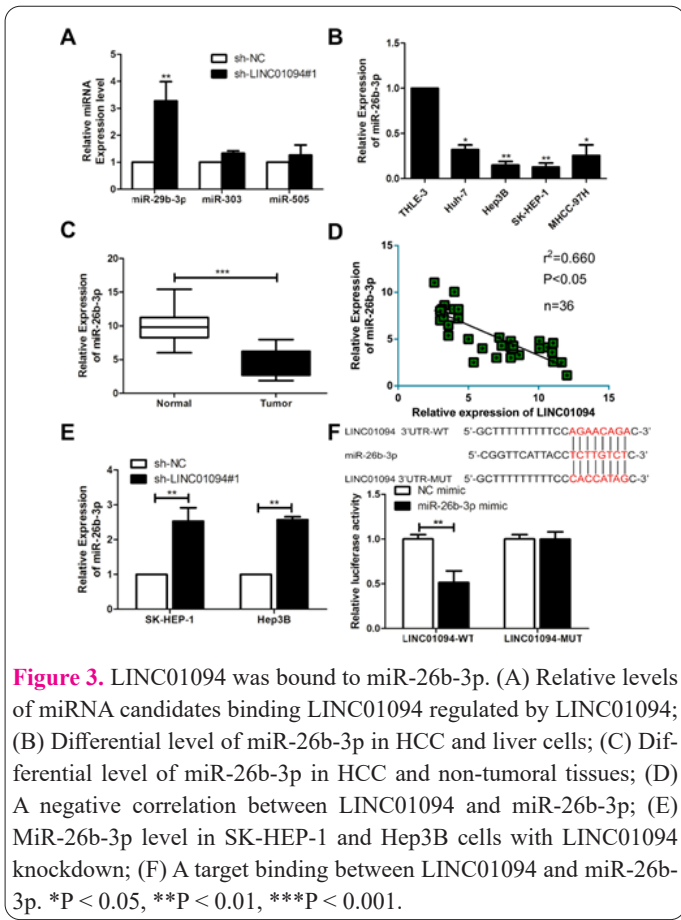


Figure 3. LINC01094 was bound to miR-26b-3p. (A) Relative levels of miRNA candidates binding LINC01094 regulated by LINC01094; (B) Differential level of miR-26b-3p in HCC and liver cells; (C) Differential level of miR-26b-3p in HCC and non-tumoral tissues; (D) A negative correlation between LINC01094 and miR-26b-3p; (E) MiR-26b-3p level in SK-HEP-1 and Hep3B cells with LINC01094 knockdown; (F) A target binding between LINC01094 and miR-26b-3p. *P < 0.05, **P < 0.01, ***P < 0.001.

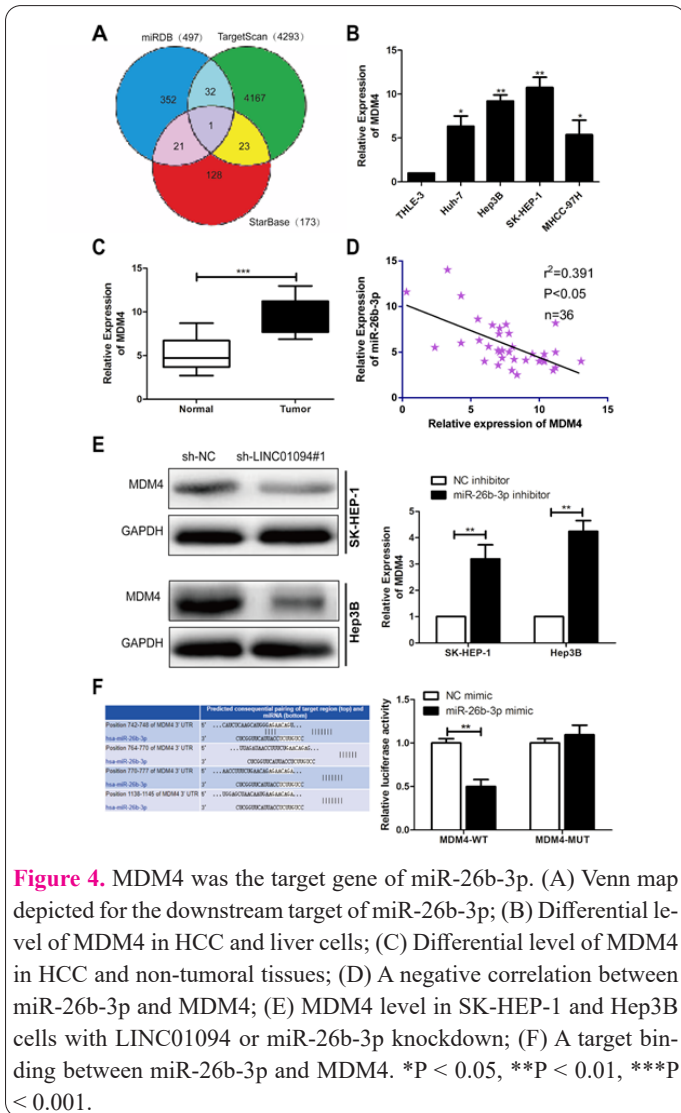


Figure 4. MDM4 was the target gene of miR-26b-3p. (A) Venn map depicted for the downstream target of miR-26b-3p; (B) Differential level of MDM4 in HCC and liver cells; (C) Differential level of MDM4 in HCC and non-tumoral tissues; (D) A negative correlation between miR-26b-3p and MDM4; (E) MDM4 level in SK-HEP-1 and Hep3B cells with LINC01094 or miR-26b-3p knockdown; (F) A target binding between miR-26b-3p and MDM4. *P < 0.05, **P < 0.01, ***P < 0.001.

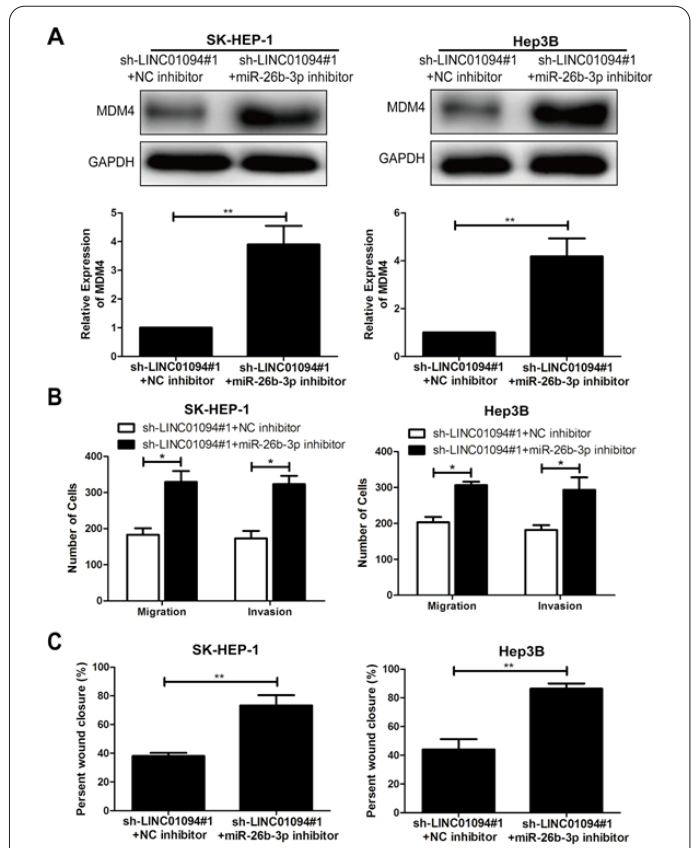


Figure 5. LINC01094 regulated HCC cell metastasis via the miR-26b-3p/MDM4 axis. (A) MDM4 level in SK-HEP-1 and Hep3B cells with co-silence of LINC01094 and miR-26b-3p; (B) Migration and invasion in SK-HEP-1 and Hep3B cells with co-silence of LINC01094 and miR-26b-3p (magnification 20×); (C) Wound closure in SK-HEP-1 and Hep3B cells with co-silence of LINC01094 and miR-26b-3p. *P < 0.05.

target gene of miR-26b-3p (Figure 4F).

LINC01094 regulated HCC cell metastasis via miR-26b-3p/MDM4 axis

To further illustrate the interaction between LINC01094 and the miR-26b-3p/MDM4 axis in HCC progression, co-transfection of sh-LINC01094#1 and miR-26b-3p inhibitor was conducted. The protein level of MDM4 was higher in SK-HEP-1 and Hep3B cells with co-silence of LINC01094 and miR-26b-3p than those with silence of LINC01094 only (Figure 5A). In addition, migratory and invasive rates were higher in HCC cells co-transfected with sh-LINC01094#1 and miR-26b-3p inhibitor in comparison to those co-transfected with sh-LINC01094#1 and NC inhibitor (Figure 5B, 5C).

Discussion

HCC is a malignant tumor with strong invasiveness, high metastasis, and poor prognosis. It causes the third highest cancer-related death in the world (1-3). Despite the continuous improvement of medical technology, there are more than 250,000 new cases and 600,000 deaths of HCC each year (2,4-6). The specific molecular mechanism underlying HCC remains largely unclear (6,7). Therefore, finding new biological indicators for early diagnosis and predicting the prognosis of HCC is of great significance (8,9).

LncRNAs are a type of endogenous RNAs that barely

encode proteins. They often have a poly(A) tail, accounting for about 80% of non-coding RNAs (10-12). They are initially considered to be non-functional by-products of RNA polymerase II transcription (13,14). With the deepening of research, it is found that lncRNAs not only participate in the normal physiological activities of cells but also have a relation to the pathogenesis of multiple tumors (14-16). Jiang et al. (17) reported that LINC01094 induces the deterioration of ccRCC through the miR-224-5p/CHSY1 axis, and it predicts a poor prognosis. Our findings uncovered that LINC01094 was upregulated in clinical samples of HCC and cell lines, suggesting its oncogenic role. Later, *in vitro*, experiments obtained the conclusion that LINC01094 stimulated migratory and invasive potentials in HCC cells.

The discovery of lncRNAs and exploration of their biological functions gradually reveal their potential as tumor biomarkers (14,16). Typically, lncRNAs act as competitive endogenous RNAs to block the regulation of target miRNAs on their downstream genes, thereby affecting cell functions (19-23). Based on the predicted binding sites and verification by dual-luciferase reporter assay, we identified a feedback loop LINC01094/miR-26b-3p/MDM4. In particular, LINC01094 exerted a miRNA sponge effect on miR-26b-3p and thus blocked the role of miR-26b-3p in inhibiting the expression level of MDM4. Moreover, rescue experiments indicated that the knockdown of miR-26b-3p could reverse the inhibited metastasis in Hep3B and SK-HEP-1 cells with a stable knockdown of LINC01094. It is concluded that LINC01094 exerted an oncogenic role in triggering HCC metastasis *via* the miR-26b-3p/MDM4 axis.

LINC01094 accelerates the metastasis of HCC *via* the miR-26b-3p/MDM4 axis, which is a potential biomarker and therapeutic target to be utilized in clinical practice.

Conflict of Interest

The authors declared no conflict of interest.

References

1. El-Serag HB, Rudolph KL. Hepatocellular carcinoma: epidemiology and molecular carcinogenesis. *Gastroenterology* 2007; 132(7): 2557-2576.
2. Clark T, Maximin S, Meier J, Pokharel S, Bhargava P. Hepatocellular Carcinoma: Review of Epidemiology, Screening, Imaging Diagnosis, Response Assessment, and Treatment. *Curr Probl Diagn Rad* 2015; 44(6): 479-486.
3. Massarweh NN, El-Serag HB. Epidemiology of Hepatocellular Carcinoma and Intrahepatic Cholangiocarcinoma. *Cancer Control* 2017; 24(3): 1145164509.
4. McGlynn KA, Petrick JL, El-Serag HB. Epidemiology of Hepatocellular Carcinoma. *Hepatology* 2021; 73 Suppl 1(Suppl 1): 4-13.
5. Li H, Niu X, Zhang D, Qu MH, Yang K. The role of the canonical nf-kappab signaling pathway in the development of acute liver failure. *Biotechnol Genet Eng* 2022: 1-21.
6. Grandhi MS, Kim AK, Ronnekleiv-Kelly SM, Kamel IR, Ghasebeh MA, Pawlik TM. Hepatocellular carcinoma: From diagnosis to treatment. *Surg Oncol* 2016; 25(2): 74-85.
7. Lurje I, Czigany Z, Bednarsch J, et al. Treatment Strategies for Hepatocellular Carcinoma (-) a Multidisciplinary Approach. *Int J Mol Sci* 2019; 20(6): 1465.
8. El JT, Lagana SM, Lee H. Update on hepatocellular carcinoma: Pathologists' review. *World J Gastroentero* 2019; 25(14): 1653-1665.
9. Khemlina G, Ikeda S, Kurzrock R. The biology of Hepatocellular carcinoma: implications for genomic and immune therapies. *Mol Cancer* 2017; 16(1): 149.
10. Ito KK, Watanabe K, Kitagawa D. The Emerging Role of ncRNAs and RNA-Binding Proteins in Mitotic Apparatus Formation. *Non-Coding Rna* 2020; 6(1): 13.
11. Budak H, Kaya SB, Cagirici HB. Long Non-coding RNA in Plants in the Era of Reference Sequences. *Front Plant Sci* 2020; 11: 276.
12. Xu J, Bai J, Xiao J. Computationally Modeling ncRNA-ncRNA Crosstalk. *Adv Exp Med Biol* 2018; 1094: 77-86.
13. Nigita G, Marceca GP, Tomasello L, et al. ncRNA Editing: Functional Characterization and Computational Resources. *Methods Mol Biol* 2019; 1912: 133-174.
14. Jathar S, Kumar V, Srivastava J, Tripathi V. Technological Developments in lncRNA Biology. *Adv Exp Med Biol* 2017; 1008: 283-323.
15. Kuo TC, Kung HJ, Shih JW. Signaling in and out: long-noncoding RNAs in tumor hypoxia. *J Biomed Sci* 2020; 27(1): 59.
16. Kopp F, Mendell JT. Functional Classification and Experimental Dissection of Long Noncoding RNAs. *Cell* 2018; 172(3): 393-407.
17. Jiang Y, Zhang H, Li W, Yan Y, Yao X, Gu W. FOXM1-Activated LINC01094 Promotes Clear Cell Renal Cell Carcinoma Development via MicroRNA 224-5p/CHSY1. *Mol Cell Biol* 2020; 40(3): e00357-19.
18. Fei Q, Bai X, Lin J, Meng H, Yang Y, Guo A. Identification of aberrantly expressed long non-coding RNAs in postmenopausal osteoporosis. *Int J Mol Med* 2018; 41(6): 3537-3550.
19. Geng F, Lu GF, Ji MH, et al. MicroRNA-26b-3p/ANTXR1 signaling modulates proliferation, migration, and apoptosis of glioma. *Am J Transl Res* 2019; 11(12): 7568-7578.
20. Malik S, Prasad S, Kishore S, Kumar A, Upadhyay V. A perspective review on impact and molecular mechanism of environmental carcinogens on human health. *Biotechnol Genet Eng* 2021; 37(2): 178-207.
21. Liu T, Zhang H, Yi S, Gu L, Zhou M. Mutual regulation of MDM4 and TOP2A in cancer cell proliferation. *Mol Oncol* 2019; 13(5): 1047-1058.
22. Azizi Dargahlou, S., Iriti, M., Pouresmaeil, M., Goh, L. P. W. MicroRNAs; their therapeutic and biomarker properties. *Cell Mol Biomed Rep* 2023; 3(2): 73-88. doi: 10.55705/cnbr.2022.365396.1085
23. Kanwal, N., Al Samarrai, O., Al-Zaidi, H. M. H., Mirzaei, A., Heidari, M. Comprehensive analysis of microRNA (miRNA) in cancer cells. *Cell Mol Biomed Rep* 2023; 3(2): 89-97. doi: 10.55705/cnbr.2022.364591.1070.